Carbohydrate Polymers 89 (2012) 906–913

Contents lists available at SciVerse ScienceDirect

Carbohydrate Polymers

journal homepage: www.elsevier.com/locate/carbpol

Silver nanoparticle-loaded PVA/gum acacia hydrogel: Synthesis, characterization and antibacterial study

K.A. Juby[a], Charu Dwivedi[a], Manmohan Kumar[a,*], Swathi Kota[b], H.S. Misra[b], P.N. Bajaj[a]

[a] Radiation and Photochemistry Division, Bhabha Atomic Research Centre, Trombay, Mumbai 400085, India
[b] Molecular Biology Division, Bhabha Atomic Research Centre, Trombay, Mumbai 400085, India

ARTICLE INFO

Article history:
Received 6 March 2012
Received in revised form 2 April 2012
Accepted 10 April 2012
Available online 20 April 2012

Keywords:
Polyvinyl alcohol
Gum acacia
Hydrogel
Gamma irradiation
Silver nanoparticle
Antibacterial

ABSTRACT

A simple one-pot method for in situ synthesis of silver nanoparticles (AgNPs), within polyvinyl alcohol/gum acacia (PVA–GA) hydrogel matrix, by gamma radiation-induced cross-linking is reported here. The synthesized hydrogels were characterized by FT-IR, thermogravimetry, dynamic light scattering and inductively coupled mass spectrometry method. The thermal stability was found to be more for the hydrogel loaded with silver nanoparticles and also the percentage silver loading was found to increase with increase in cross-linking density. The influence of gum acacia (GA) concentration on the equilibrium degree of swelling of the synthesized hydrogels, and also on the silver release from hydrogel matrix, was investigated. The size of the silver nanoparticles formed in the hydrogel matrix was in the range of 10–40 nm. The rheological gel point was found to be at 25.34 kGy of radiation dose, for a typical hydrogel synthesized, using 5% GA, 3% PVA and 1 mM $AgNO_3$. The antibacterial studies of the synthesized nanosilver-containing hydrogels showed good antibacterial activity against gram-negative bacterium, *Escherichia coli*.

1. Introduction

Metal nanoparticles-embedded hydrogels, wherein the three dimensional, hydrophilic polymeric network stabilizes the nanoparticles, have attracted attention these days mainly due to their wide range of applications in the field of catalysis, biomedicine, optics, pharmaceuticals, etc. (Jovanović et al., 2011). A variety of hydrogel matrices based on various natural polymers, or their derivatives, like starch, gelatin, chitosan, carboxy methyl cellulose, sodium alginate, etc., along with synthetic polymers, like polyvinyl alcohol (PVA), polyvinyl pyrollidone (PVP), etc., have been developed (Bajpai, Mohan, Bajpai, Tankhiwale, & Thomas, 2007; Kong & Jang, 2008; Sharma, Yongard, & Lin, 2009; Thomas, Mohan, Sreedhar, & Bajpai, 2009; Thomas, Namdeo, Mohan, Bajpai, & Bajpai, 2008; Vimala, Sivudu, Mohan, Sreedhar, & Raju, 2009). Among the different metal nanoparticles, most of the studies have been performed with noble metals, like silver and gold. But, most of the synthetic routes for the formation of metal nanoparticles employ chemical reduction methods, using hydrazine hydrate, dimethyl formamide, ethylene glycol, etc., which cause toxicity and biological hazards. Recent research efforts in this area are directed more towards developing new approaches, to incorporate metal nanoparticles into polymeric hydrogel matrices, without involving any toxic chemical reductants, or using any complicated physical techniques, such as sputtering, plasma deposition, etc. (Jovanović et al., 2011). Radiation technology is one such method, by which it is possible to synthesize nanoparticles, in situ in the hydrogel matrix.

The advantage of the radiation-induced synthesis of hydrogels is that, the process can be optimized to form a sterilized gel matrix, and hence, can be used, without further purification, for various biomedical applications (Varshney, 2007). In addition to this, radiation-induced method for synthesis of nanoparticles has a better control over the size (Jovanović et al., 2011). Hence, at the outset, radiation technique can be used as a cleaner and simpler method, to form a hydrogel matrix, with nanoparticles embedded in it.

While considering the synthesis of hydrogels, its biocompatibility is an important parameter for biomedical applications. Synthesis of biocompatible hydrogel matrix from a nontoxic, economical, and easily available materials, such as polysaccharides, is more advantageous than that from synthetic polymers (Sharma et al., 2009). Gum acacia (GA) is a well-known polysaccharide, obtained from the stems and branches of Acacia Senegal tree (Dror, Cohen, & Yerushalmi-Rozen, 2006; Rao et al., 2010; Renard, Lavenant-Gourgeon, Ralet, & Sanchez, 2006). According to the recent structural studies, it is known to be composed of (i) arabinogalactan, (ii) arabinogalactam–protein (AGP) complex fraction

* Corresponding author. Tel.: +91 22 25593994; fax: +91 22 25505151.
E-mail address: manmoku@barc.gov.in (M. Kumar).

0144-8617/$ – see front matter © 2012 Elsevier Ltd. All rights reserved.
http://dx.doi.org/10.1016/j.carbpol.2012.04.033

and (iii) minor glycoprotein fraction. The high molecular weight protein part in GA is attached to polysaccharide through hydroxyproline and serine residues. Uronic acid (16%) is present, in low quantities, in different components of the gum, which makes it a weakly charged polyelectrolyte (Dror et al., 2006; Rao et al., 2010). But, GA cannot be cross-linked by gamma-irradiation, whereas PVA is well known for formation of hydrogels, induced by gamma, as well as electron irradiation. The highly biocompatible, economical and environmental friendly nature of both gum acacia and PVA make these obvious choice for the synthesis of a composite hydrogel matrix.

Thus, a combination of water soluble biopolymer GA and synthetic polymer PVA with silver nanoparticles (AgNPs) can produce new hydrogel matrix, with antimicrobial property. Recent studies have shown that, silver, in the form of nanoparticles, is very effective as antimicrobial agent, both in vivo and in vitro, as compared to bulk silver, or silver ions, due to their enhanced permeation and retention effects (Francis, Varshney, & Kumar, 2004; Kora, Sashidhar, & Arunachalam, 2010; Lu, Gao, & Gu, 2008; Malý, Lampová, Semerádtová, Štofik, & Kováčik, 2009; Mohan, Raju, Sambasivudu, Singh, & Sreedhar, 2007; Vimala et al., 2011). Their antimicrobial activity is due to the interaction with sulfur containing proteins present in bacterial cell membrane, as well as with phosphorous containing DNA.

The size and the rate of leaching of the AgNPs can play a major role in antimicrobial activity of these hydrogels, especially for wound dressing applications. In such applications, a hydrophilic environment is necessary, to facilitate the release of silver from the polymer matrix, and also to maintain a moist environment around the wound bed, which is essential for optimal wound healing. The polysaccharides, like gum acacia, carrageenan, agar, etc., improve the water retention properties, making these suitable for hydrogel synthesis.

In the present work, in view of the advantages of radiation technique and biocompatibility of the hydrogel matrix, radiolytic synthesis of silver nanoparticle-loaded PVA–GA hydrogel (Ag/PVA–GA hydrogel) has been carried out, and the results of its antibacterial study are presented.

2. Materials and methods

2.1. Materials

Silver nitrate (Merck), gum acacia (S D Fine Chemicals) and polyvinyl alcohol (Mw approximately 125,000, S D Fine Chemicals) were used in the synthesis of hydrogels. All these chemicals were of analytical grade, and were used, without further purification. LB agar, used for antibacterial studies, was obtained from Hi media Laboratories. Water, with conductivity 0.6 $\mu S\,cm^{-1}$, from Millipore Milli-Q system, was used for the preparation of aqueous solutions.

2.2. Preparation of Ag/PVA–GA composite hydrogel

For preparation of PVA–GA blends, freshly prepared stocks of 10% PVA and 10% GA (by weight %) in water were used. Aqueous 3% PVA blends, containing different concentrations of GA (1%, 2%, 3%, and 5%) and 1 mM $AgNO_3$, were prepared by appropriate dilution of these stock solutions. The PVA–GA blends, containing $AgNO_3$, were transferred into glass tubes and deoxygenated with nitrogen, for 30 min, at 5 ml/min, and the tubes were sealed. The tubes were irradiated in Co-60 γ-source at a dose rate of 1.32 kGy/h, to an absorbed dose of 32 kGy, under ambient conditions. While for gel point determination study, the hydrogels were formed by irradiating the solutions to different doses. The synthesized Ag/PVA–GA hydrogels were taken out, and washed thoroughly with distilled water, to remove the unreacted species. These gels were dried under vaccum, at 40 °C, to constant weight, for further characterization by different techniques.

3. Experimental

3.1. FT-IR analysis

The IR spectra were recorded on diamond single reflectance ATR in IR Affinity-1 spectrometer. The dried Ag/PVA–GA hydrogel samples were analyzed, to study the structure of the hydrogels.

3.2. Thermogravimetric analysis (TGA)

Thermogravimetric analysis was performed, using Mettler Toledo TG/DSC star^e system. About 5–10 mg of the dried hydrogel samples were heated in an alumina crucible, and the profiles were recorded from 30 to 750 °C, at a scan rate of 10 °C/min, under nitrogen atmosphere, with a flow rate of 50 ml/min (Varaprasad, Mohan, Vimala, & Raju, 2011). The thermal stability of the hydrogel matrix was studied, using the thermogravimetric data.

3.3. ICP-MS analysis

The amount of AgNPs loaded in the hydrogel matrix was determined by VG PQ Ex Cell (Thermo Elemental) inductively coupled mass spectrometry (ICP-MS). Also, the influence of GA concentration on the extent of silver loading was studied by this method.

3.4. Equilibrium degree of swelling

Equilibrium degree of swelling (EDS) was determined gravimetrically. The hydrogel samples dried to constant weight were immersed in the water at room temperature, for ~24 h. The excess water was removed with a filter paper and the samples were weighed. The EDS% was calculated, using the following equation:

$$\text{EDS\%} = \frac{W_e - W_d}{W_d} \times 100 \quad (1)$$

where, W_e is weight of the swollen hydrogel at equilibrium and W_d is initial weight of the dried hydrogel.

The EDS% values were determined at different pH values and compositions of the hydrogel. The pH was adjusted to the desired value, by using 0.1 M HCl and 0.1 M NaOH solutions, with the ionic strength maintained at 0.1 M, with sodium chloride.

3.5. Release of silver from hydrogels

In vitro release profiles of silver from hydrogel matrices were obtained, by measuring optical density (O.D.) at different time periods. Briefly, hydrogel pieces weighing ~1.0 g were stored in a flask, containing 10 ml of water at 37 °C, and the flask was oscillated at a frequency of 60 rpm in a rotary shaker. Amount of the silver released was determined, by measuring O.D. at λ_{max} (420 nm), using Jasco V-650 spectrophotometer.

3.6. Particle size analysis

Particle size analysis was carried out by dynamic light scattering (DLS) method, using VASCO γ particle size analyzer at 25 °C (laser wavelength 658 nm). DLS method measures the Rayleigh scattering based on the assumptions of spherical shape and monomodal size distribution of the particles (Mahl, Diendorf, Meyer-Zaika, & Epple, 2011). The variation in the average particle size of AgNPs, with change in GA concentration, was studied.

3.7. Rheological measurements

The rheological measurements were carried out, using the parallel plate geometry (Anton Paar physica MCR101; PP25-4, diameter 24.972 mm). Gel point determination studies were carried out by frequency sweep tests at 25 °C. All the dynamic measurements were performed in the linear viscoelastic region. Viscoelastic properties were measured in 0.1–100 rad/s frequency range. The viscoelastic functions recorded during gelation were the elastic $G'(\omega)$ and viscous $G''(\omega)$ moduli, as well as the damping factor $\tan(\delta)$, which is defined as $G''(\omega)/G'(\omega)$.

3.8. Antibacterial studies

Antibacterial activity of the swollen Ag/PVA–GA blend hydrogels obtained directly after γ-irradiation (without any washing or drying) against wild type *Escherichia coli* W1103 (*E. coli*) (gram negative) was evaluated, using the disc diffusion method (Varaprasad et al., 2011; Vimala et al., 2011). Overnight grown culture of *E. coli* was diluted, and plated on LB agar. Equally weighed hydrogel samples, consisting of different compositions, were kept on the plates and incubated at 37 °C for 18 h. The plates were taken out, and the inhibition area was observed.

4. Results and discussion

Exposure of an aqueous solution to γ-irradiation mainly produces OH•, H• radicals and hydrated electrons (e_{aq}^-), along with some molecular products, due to radiolysis of solvent, as shown below (2).

$$H_2O \xrightarrow{\gamma\text{-radiation}} e_{aq}^-, H^\bullet, OH^\bullet, H_3O^+, H_2, H_2O_2 \quad (2)$$

Among these, OH• is oxidizing in nature, while H• and e_{aq}^- are of reducing nature. The OH• and H• radicals are mainly responsible for crosslinking/degradation of the polymeric solutes, whereas H• and e_{aq}^- reduce Ag^+ ions to AgNPs (3). These neutral Ag^0 atoms combine with the excess Ag^+ ions, trapped in the polymer chains, and lead to the formation of dimeric clusters of silver (4).

$$Ag^+ + e_{aq}^-/H^\bullet \rightarrow Ag^0 + H_2O/H^+ \quad (3)$$

$$Ag^0 + Ag^+ \rightarrow Ag_2^+ \quad (4)$$

The dimeric clusters thus formed can further react with excess silver cations, to form trimeric, tetrameric and higher order silver clusters on subsequent reduction. These higher clusters grow with time to form nanoparticles which get stabilized in the nano level domains of PVA–GA matrix. These nano level domains are formed due to inter- and intra-molecular cross linking of GA and PVA polymer chains, providing a hydrogel network system. The clusters trapped in these domains convert themselves into nanoparticles, on continuous irradiation. The oxygen atoms of the functional groups on the network chains anchor the AgNPs, resulting in a surface charge. This leads to an electrostatic repulsive force, which along with the steric effects of the polymer chains, stabilizes the nanoparticles (Rao et al., 2010; Thomas et al., 2008).

A polymer may cross-link, or degrade, on irradiation, depending on its chemical structure. PVA is known to be a cross-linking polymer, while GA is of degrading nature. Therefore, along with cross-linking of PVA, degradation of polysaccharide GA also takes place in the reaction medium, and the overall behavior will depend on the relative concentrations of the two polymers (Varshney, 2007).

The rate constants for reaction of OH• and H• radicals with both PVA and GA are very similar, and are of the order of 10^9 dm^3 mol^{-1} s^{-1}, while the rate constants for the reaction of e_{aq}^- with both these polymers are much lower. On the contrary, reactivity of both OH• and e_{aq}^- with Ag^+ ions are about an order of magnitude higher (i.e., 10^{10} dm^3 mol^{-1} s^{-1}). The concentrations of the solutes are appropriately chosen, so that the OH• and H• radicals preferentially react with the polymers, and the e_{aq}^- reacts mostly with Ag^+ ions, leading to a cross-linked hydrogel network, containing AgNPs (Kumar, Varshney, & Francis, 2005). Thus, an aqueous solution of PVA, GA and silver nitrate of appropriate concentrations crosslinks, on gamma irradiation, to form yellow-colored gel, with AgNPs trapped in the network. The parameters, like gel strength, water absorption capacity, thermal strength, adhesion, etc., depend on the concentrations of PVA and GA, cross-linking density, gamma dose, irradiation conditions, etc.

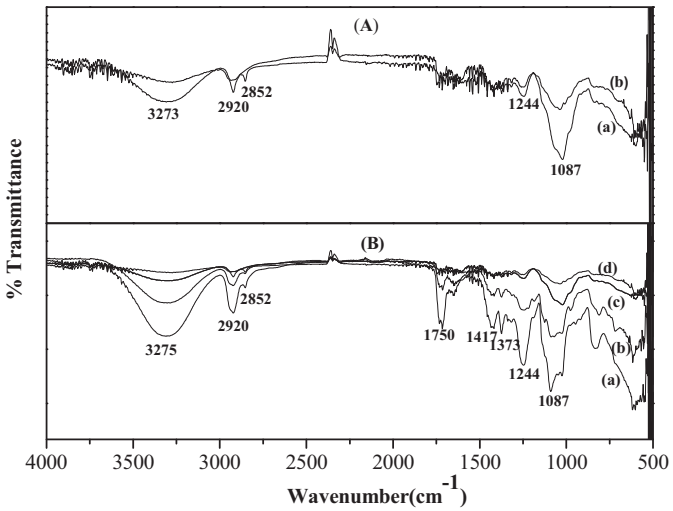

Fig. 1. FT-IR spectra of vaccum-dried hydrogel samples: (A) Synthesized from solution containing 5% GA and 3% PVA (a) without AgNPs, (b) with AgNPs. (B) Synthesized, using variable GA concentration, (a) 0%, (b) 1%, (c) 3%, (d) 5% with 3% PVA, 1 mM $AgNO_3$, and a radiation dose of 32 kGy.

4.1. Characterization of Ag/PVA–GA hydrogels

4.1.1. FT-IR analysis

The FT-IR spectra of PVA–GA and Ag/PVA–GA hydrogel samples were recorded, in order to identify the functional groups involved in the synthesis of AgNPs. In the presence of silver, the oxygen atoms of —OH and —COOH groups get associated with silver clusters (Mohan et al., 2007). This leads to broadening and shifting of O—H stretching from 3273 cm^{-1} (silver unloaded) to 3258 cm^{-1} (silver loaded). The bands at 2920 and 2852 cm^{-1} correspond to asymmetric and symmetric C—H stretching, respectively (Fig. 1A) (Kora et al., 2010).

FT-IR spectra of silver-loaded hydrogel samples, containing different concentrations of GA (0%, 1%, 3%, and 5%), were also recorded, to understand the variation in the interaction between GA, PVA and silver (Fig. 1B). The major peaks are 3275 cm^{-1} (O—H stretching), 2920 cm^{-1}, 2852 cm^{-1} (C—H stretching), 1750 cm^{-1} (C=O stretching of PVA and GA), 1417 cm^{-1} (O—H deformation), 1244 cm^{-1} (C—O stretching of PVA) and 1087 cm^{-1} (C—OH stretching of GA) (Rao et al., 2010). The presence of a large number of hydroxyl and carboxyl groups, and the possible hydrogen bonding between them resulted in broadening of the peaks at ~3200 cm^{-1} and ~1000 cm^{-1}. With increase in the concentration of GA, more hydroxyl groups are involved in hydrogen bonding, and this leads to further peak broadening and slight shift in the C—O stretching frequency of PVA at 1244 cm^{-1}, as well as that of GA at 1087 cm^{-1} (Fig. 1B).

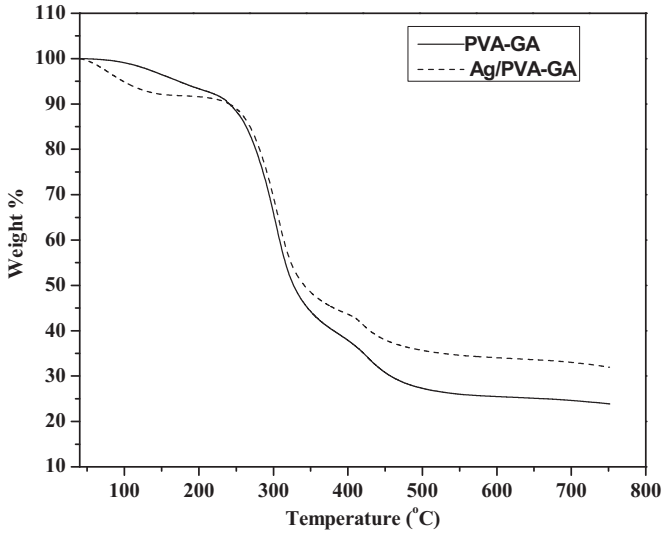

Fig. 2. Thermogravimetric profiles showing the weight loss in (PVA–GA) and (Ag/PVA–GA) vacuum-dried hydrogel samples.

4.1.2. Thermogravimetric analysis

The thermal stability of silver-loaded hydrogel was determined by thermogravimetric analysis. Fig. 2 illustrates the thermogram of silver-loaded and unloaded dry hydrogel samples. The weight loss observed for PVA–GA hydrogel sample up to 500 °C is 72.69%, whereas Ag/PVA–GA hydrogel shows only 64.34% at the same temperature. The observed difference in the weight loss is much more than the expected weight of AgNPs present in the hydrogel.

The increase in thermal stability of the silver nanoparticles-loaded hydrogel, as indicated by the results of the TGA study, can be due to two reasons. AgNPs have higher thermal stability as compared to the polymeric chains of the hydrogel. Hence, the presence of AgNPs in the system may make it thermally more stable. But, the small change in the composition of the hydrogel matrix, due to the presence of only about 0.14 wt% of AgNPs, cannot account for the observed change in the thermal stability. The other reason for this change could be the reduced mobility of the polymeric chains on loading of silver nanoparticles, leading to the enhanced thermal stability. The silver nanoparticles/clusters interact with PVA and GA through the —COOH and —OH groups present in the polymeric chains, as indicated by the results of the FT-IR study. Such interactions can lead to formation of some weak intermolecular cross-links between the polymeric chains, thereby restricting their mobility. Consequently, the degradation process will be slowed down, and the decomposition takes place at higher temperature in the presence of AgNPs (Mbhele et al., 2003).

4.1.3. Determination of AgNPs in the hydrogel matrix

The dried hydrogel samples made from aqueous solutions, with different GA concentrations (1%, 2%, 3%, and 5%), constant PVA (3%) and $AgNO_3$ (1 mM), were weighed accurately, and dissolved in conc. HNO_3, so that all the AgNPs in the matrix get oxidized to Ag^+. The solutions were diluted appropriately, and the silver ions in the solution were analyzed by ICP-MS method. It was observed that the silver ion concentration was less in the sample with more GA fraction, and it increased with increase in PVA fraction in the hydrogel matrix. These results suggest that, AgNPs loading in the hydrogel matrix increases with increase in cross-linking density. This may be, because the Ag^+ ions interact more strongly with PVA chains as compared to GA, leading to higher loading of AgNPs in the hydrogels, having higher PVA fractions.

Table 1A
Variation in EDS% of the hydrogels synthesized at different PVA and GA concentrations in the presence of 1 mM $AgNO_3$, at radiation dose of 32 kGy.

PVA (wt%)	GA (wt%)	GA fraction	EDS%[a]
5	0	0.0	984
5	2	0.3	1170
5	3	0.4	1390
3	5	0.5	1553
3	5	0.6	1830

[a] Average of three measurements.

Table 1B
Effect of pH on the EDS% of the hydrogel, formed by γ-irradiation of aqueous solution, containing 3% PVA, 5% GA, and 1 mM $AgNO_3$, for 32 kGy dose.

pH	EDS%[a]
1	1424
4	1485
7	1466
10	1489
12	Gel disintegrated

[a] Average of three measurements.

4.2. Swelling studies of the hydrogels

4.2.1. Equilibrium degree of swelling as a function of PVA and GA concentration

The EDS% of the hydrogels formed was determined for different concentrations of PVA and GA, keeping concentration of silver nitrate and the radiation dose constant, to study the effect of this variation, on the network structure of the hydrogels. It is observed that there is increase in EDS% with the increase in the fraction of GA in the hydrogel matrix (Table 1A). This is because, at higher PVA concentrations, cross-linking density is more, resulting in a tighter 3D-structure, which will swell less, in comparison to the hydrogels, with lower cross-linking ratios. Gel formation was not observed, at radiation dose of 32 kGy, when the PVA concentration was below 3%, and GA concentration was above 5%.

The hydrophilic nature of GA causes more hydrogen bonding between the gum molecules and water, and leads to increase in the EDS%. This can also be explained in terms of decrease in the crystallinity of PVA segments, due to the bulky units of GA. In fact, the hydrogen bonding due to —OH groups crystallizes PVA through physical cross-linking, but the steric hindrance of the bulky GA groups disturbs the chains, and decreases the crystallinity. Also, the presence of GA in polymer solution reduces the probability of radical combination during irradiation, which reduces the cross-linking density of the gel. This leads to more free volumes in the polymer network, and consequently, more water can be absorbed (Francis et al., 2004).

4.2.2. Equilibrium degree of swelling as a function of pH

pH sensitivity of the matrix was analyzed, by determining EDS% at different pH values of the absorbing medium. The EDS% does not vary significantly with variation in pH of the medium (Table 1B). This behavior may be because, the pH dependent —COOH groups of GA are very less as compared to the —OH groups present in PVA and GA together. Hence, the pH variation does not significantly affect EDS% of the hydrogels. The hydrogel was found to be unstable under alkaline conditions (above pH 12).

4.3. Release of silver from hydrogels

The antimicrobial activity of silver containing hydrogels is dependent on the release of silver from the polymeric matrix to the pathogenic environment. UV–vis spectroscopic technique was utilized, to study the leaching of silver. Freshly prepared Ag/PVA–GA

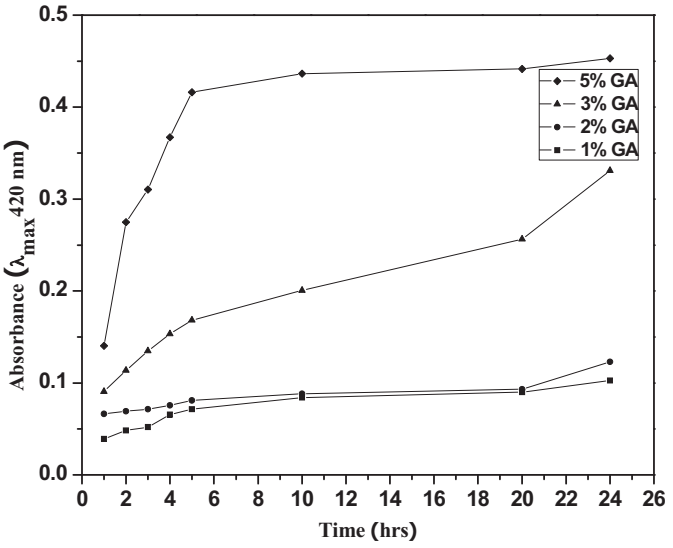

Fig. 3. Graph showing the silver release profiles of hydrogels, prepared with different GA concentrations, 3% PVA, 1 mM $AgNO_3$, and radiation dose of 32 kGy.

hydrogel samples, with different initial GA contents, 1%, 2%, 3%, and 5% (w/v), were used for the investigation. As shown in Fig. 3, in the case of 5% GA sample, the release of silver is rapid in the beginning, and then, it becomes almost constant. This is probably due to higher hydrophilicity of the matrix with increasing GA concentration. Lowering the concentration of GA (1%, 2%, and 3%) decreased the initial rate of release. A considerable increase can be observed only after long incubation period of ~20 h. The longer time for the release of silver may be the result of slow swelling nature of the matrix with low GA content.

4.4. Particle size analysis

The variation in AgNPs size distribution was studied as a function of GA concentration, keeping the radiation dose (32 kGy), PVA (3%) and silver ion concentration (1 mM) constant. The mean particle diameters, when GA concentration was 1%, 2%, 3% and 5%, was obtained as 9.8, 13.7, 16.9 and 42.0 nm, respectively (Fig. 4). This may be because, with increase in GA concentration, the possibility of inter- and intra-molecular crosslinking in PVA decreases as a result of steric effects due to GA, and hence, the cross-linking density decreases. So, there is more probability of aggregation of silver nanoparticles in the matrix, resulting in larger clusters of nanoparticles.

4.5. Rheological study for gel point determination

Gelation is a process which involves change from liquid to solid-like behavior. This can be studied by rheological experiments. The storage modulus $G'(\omega)$ and the loss modulus $G''(\omega)$ can be measured, by applying an oscillatory shear field to the sample. The phase difference (δ) between the externally applied stress (σ) and strain (γ) inside the sample describes the viscoelastic properties of the material. $G' < G''$ indicates liquid-like behavior, and $G' > G''$ indicates more of solid-like behavior (Fuchs, Richtering, Burchard, Kajiwarab, & Kitamura, 1997).

The determination of gel point can be done by different rheological methods, out of which, the most reliable, and generally valid, is the one based on Chambon–Winter (CW) criterion. According to CW criterion, the gel point is indicated by the independence of the viscoelastic function, tan(δ), on frequency (ω) (Chambon, Petrovic, MacKnight, & Winter, 1986). The crossover of G' and G'' has

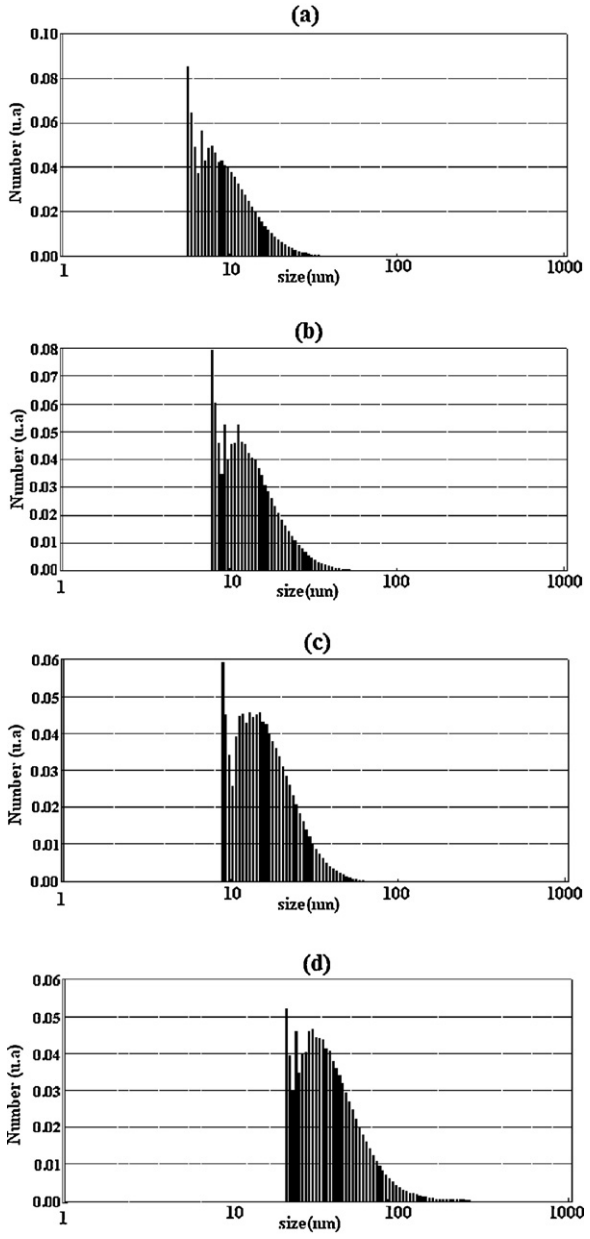

Fig. 4. Variation in particle size at different GA concentrations (a) 1%, (b) 2%, (c) 3%, and (d) 5% GA, keeping all other parameters constant.

been suggested as a criterion for gelation. However, it is frequency dependent in most of the polymer systems, and is only observable in polymer fluids, where there are permanent molecular entanglements, extending throughout the system. Also, due to 'weak gel' characteristics of the present system, observation of a crossover is perhaps not expected. Such crossovers in weak gels can be expected at lower frequencies (ω), but the experiments become unfeasible at very low frequencies, because the measurement time, t_{exp}, is inversely proportional to ω_{min}, where ω_{min} is the lowest investigated frequency (Rodd, Cooper-white, Dunstan, & Boger, 2001a). Therefore, to determine gel point (T_g) accurately, it is most appropriate to consider the point at which tan(δ) exhibits frequency independence, or alternatively, the frequency independence can be shown by the power law,

$$\tan(\delta) = K\omega^q \quad (5)$$

where, $q = 0$ at the gel point and K is a constant, which is characteristic of the gel (Rodd et al., 2001a).

The composition of the samples used for irradiation was 5% (w/v) GA, 3% (w/v) PVA and 1 mM $AgNO_3$, which was kept constant. The samples were irradiated under the same reaction conditions at different radiation doses, to study the viscoelastic properties. All the measurements were done in the linear viscoelastic region, so that the storage moduli (G') and the loss moduli (G'') were independent of the applied stress. Therefore, a stress sweep test was conducted for each sample. For the study of gelation, the storage and loss moduli were determined, from a constant stress-frequency sweep experiments over the frequency range of 0.1–100 rad/s.

Initially, for the samples obtained at lower radiation doses, $G'(\omega)$ was smaller than $G''(\omega)$, and remained small during the frequency sweep test. Then, with increase in the radiation dose, both moduli were found to increase, and finally $G'(\omega)$ became larger than $G''(\omega)$. It was observed that, above ~30 kGy radiation dose, the $G'(\omega)$ was larger than $G''(\omega)$, indicating solid-like behavior (Montembault, Viton, & Domard, 2005). Also, there is congruency of $G'(\omega)$ and $G''(\omega)$ values above ~30 kGy (Fig. 5A). But, this observation cannot give us the exact gel point.

To consider the applicability of the gel point determination method, proposed by Winter and Chambon, it is necessary to take a power law fit of tan(δ) over a range of frequencies. Fig. 5B illustrates the frequency dependence of damping factor tan(δ), at different radiation dose to the system described.

Below the gelation dose, G' increases more rapidly than G'', and thus tan(δ) decreases rapidly with dose. Initially, at lower doses, the tan(δ) value is higher at lower frequencies, which is typical for a viscoelastic liquid. This indicates that the networks are not interconnected on a macroscopic scale. After the gel point, the clusters form three dimensional interconnected networks, which is reflected by the less rapid increase of G' over G''. As a result, tan(δ) decreases gradually with dose, and increases smoothly with frequency, indicating the formation of a viscoelastic solid. After 30.2 kGy, the tan(δ) values become almost independent of frequency, suggesting the post gel point region (Montembault et al., 2005). A power law fit to the data in Fig. 5B is observed over two decades of frequency, with a correlation coefficient $R^2 \geq 0.95$.

Fitting tan(δ) to a power law relationship yields a power law coefficient (q), for each radiation dose, the relationship of which, with irradiation time, is described in Fig. 5C. The time of irradiation, at which the power law coefficient (q) passes through zero represents a frequency independent measure of tan(δ) and thus congruency in the behavior of G' and G'', fulfilling the requirements for the gel point (Rodd, Cooper-white, Dunstan, & Boger, 2001a, 2001b; Sandolo, Matricardi, Alhaique, & Coviello, 2009). From Fig. 5C it can be concluded that gel point occurs at 19.2 h of irradiation, i.e., 25.34 kGy of radiation dose.

4.6. Antibacterial studies

For checking the antibacterial activity, equally weighed hydrogel samples, containing 1%, 2%, 3% and 5% GA, keeping $AgNO_3$ and PVA concentrations constant, were subjected to disc diffusion method. After 18 h of incubation at 37 °C, inhibition zone was observed in each of the samples, which decreased with increase in GA concentration. Hydrogel samples, with 1% and 2% GA concentration, showed an inhibition zone around the sample. But, for 3% and 5% GA concentration, the gels were found to be just active by contact (Fig. 6). This is in agreement with the particle size data given in Section 4.4. So, it can be concluded that smaller the particle size the better is the antibacterial activity. Molecular basis of this inhibition is not very clear. Understanding of the mode of silver action at molecular levels can provide the assurance of silver efficacy against bacterial infections.

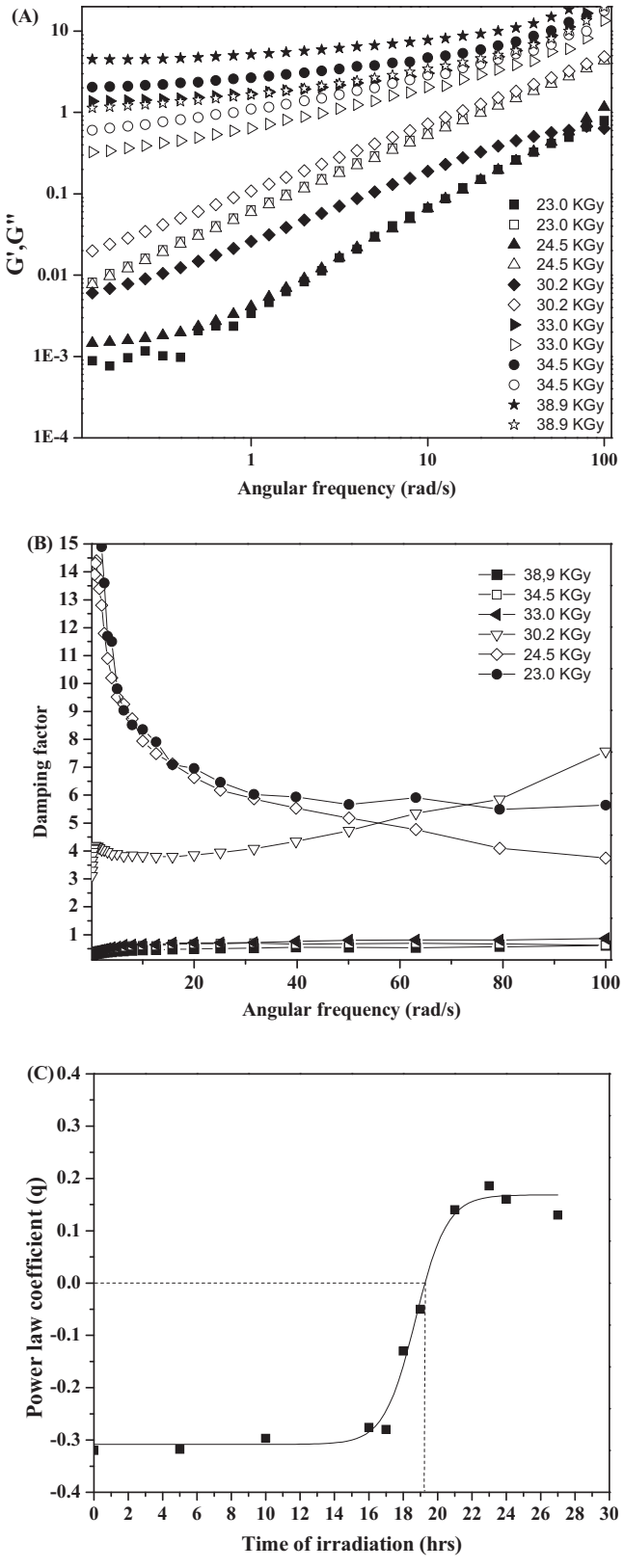

Fig. 5. (A) Frequency dependence of storage modulus G' (closed symbols) and loss modulus G'' (open symbols) at different radiation doses. (B) Frequency dependence of damping factor at different radiation doses (Only necessary data have been shown for clarity). (C) Power law coefficient (q), versus irradiation time for the samples synthesized, with 3% PVA, 5% GA and 1 mM $AgNO_3$ (all correlation coefficients for power law fit $R^2 \geq 0.95$).

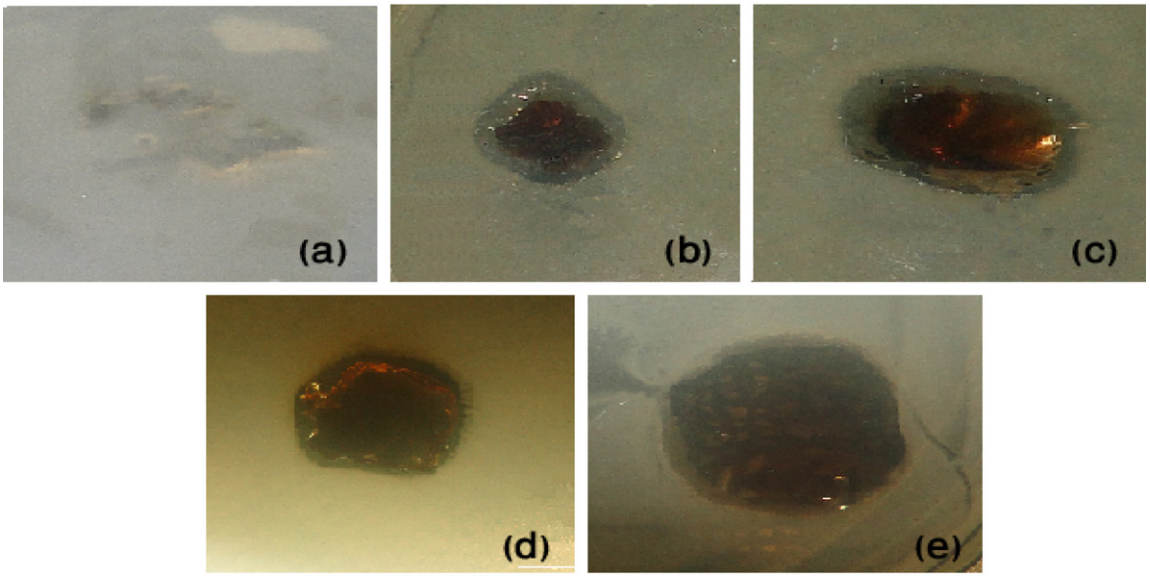

Fig. 6. Antibacterial activity picture of hydrogel samples, against *E. coli* bacteria (a) no silver loading, (b) 1% GA, (c) 2% GA, (d) 3% GA, and (e) 5% GA. All the samples were prepared with 1 mM $AgNO_3$, 3% PVA, and radiation dose of 32 kGy. (For interpretation of the references to color in this figure legend, the reader is referred to the web version of the article.)

5. Conclusion

We have reported a simple one-pot synthesis of silver nanoparticle-loaded PVA–GA hydrogel, with various size distributions (average 10–40 nm) of nanoparticles, depending on the concentration of GA, through γ-irradiation route. The addition of GA improves the biocompatibility, as well as the swelling properties of the hydrogels. The FT-IR analysis suggests that the hydroxyl and carboxylic acid functional groups, present in GA and PVA interact with AgNPs during their formation. TG analysis reveals the silver-loaded hydrogel network to be thermally more stable than the un-loaded one. Also, the silver loading is found to increase with increase in cross-linking. The swelling studies show that, the EDS% increases with increase in GA fraction, and is found to be pH independent. The silver release profiles show an increase with increase in GA concentration. The gel point determination, using CW criterion, gives the gel point at 25.34 kGy, for a typical hydrogel with 5% GA. The synthesized hydrogel shows good antibacterial performance against gram negative *E. coli* bacteria.

Acknowledgments

The authors wish to acknowledge Dr. S.K. Sarkar and Dr. T. Mukherjee, BARC, for their encouragement during the course of the study.

References

Bajpai, S. K., Mohan, Y. M., Bajpai, M., Tankhiwale, R., & Thomas, V. (2007). Synthesis of polymerstabilized silver and gold nanostructures. *Journal of Nanoscience and Nanotechnology*, *7*, 2994–3010.

Chambon, F., Petrovic, Z. S., MacKnight, W. J., & Winter, H. H. (1986). Rheology of model polyurethanes at the gel point. *Macromolecules*, *19*, 2146–2149.

Dror, Y., Cohen, Y., & Yerushalmi-Rozen, R. (2006). Structure of gum arabic in aqueous solution. *Journal of Polymer Science Part B: Polymer Physics*, *44*, 3265–3271.

Francis, S., Varshney, L., & Kumar, M. (2004). Radiation synthesis of superabsorbent poly(acrylic acid)–carrageenan hydrogels. *Radiation Physics and Chemistry*, *69*, 481–486.

Fuchs, T., Richtering, W., Burchard, W., Kajiwarab, K., & Kitamura, S. (1997). Gel point in physical gels: Rheology and light scattering from thermoreversibly gelling schizophyllan. *Polymer Gels and Networks*, *5*, 541–559.

Jovanović, Z., Krkljěs, A., Stojkovska, J., Tomić, S., Obradović, B., Mĭsković-Stanković, V., et al. (2011). Synthesis and characterization of silver/poly(N-vinyl-2-pyrrolidone) hydrogel nano composite obtained by in situ radiolytic method. *Radiation Physics and Chemistry*, *80*, 1208–1211 (and references cited therein).

Kong, H., & Jang, J. (2008). Antibacterial properties of novel poly(methyl methacrylate) nano fiber containing silver nanoparticles. *Langmuir*, *24*, 2051–2056.

Kora, A. J., Sashidhar, R. B., & Arunachalam, J. (2010). Gum kondagogu (Cochlospermum gossypium): A template for the green synthesis and stabilization of silver nanoparticles with antibacterial application. *Carbohydrate Polymers*, *82*, 670–679.

Kumar, M., Varshney, L., & Francis, S. (2005). Radiolytic formation of Ag clusters in aqueous polyvinyl alcohol solution and hydrogel matrix. *Radiation Physics and Chemistry*, *73*, 21–27.

Lu, S., Gao, W., & Gu, H. Y. (2008). Construction, application and biosafety of silver nanocrystalline chitosan wound dressing. *Burns*, *34*, 623–628.

Mahl, D., Diendorf, J., Meyer-Zaika, W., & Epple, M. (2011). Possibilities and limitations of different analytical methods for the size determination of a bimodal dispersion of metallic nanoparticles. *Colloids and Surfaces A: Physicochemical and Engineering Aspects*, *377*, 386–392.

Malý, J., Lampová, H., Semerádtová, A., Štofik, M., & Kováčik, L. (2009). The synthesis and characterization of biotin–silver–dendrimer nanocomposites as novel bioselective labels. *Nanotechnology*, *20*, 385101.

Mbhele, Z. H., Salemane, M. G., Van sitteret, C. G. C. E., Nedeljković, J. M., Djoković, V., & Luyt, A. S. (2003). Fabrication and characterization of silver–polyvinyl alcohol nanocomposites. *Chem. Mater*, *15*, 5019–5024.

Mohan, Y. M., Raju, K. M., Sambasivudu, K., Singh, S., & Sreedhar, B. (2007). Preparation of acacia-stabilized silver nanoparticles: A green approach. *Journal of Applied Polymer Science*, *106*, 3375–3381.

Montembault, A., Viton, C., & Domard, A. (2005). Rheometric study of the gelation of chitosan in a hydroalcoholic medium. *Biomaterials*, *26*, 1633–1643.

Rao, Y. N., Banerjee, D., Datta, A., Das, S. K., Guin, R., & Saha, A. (2010). Gamma irradiation route to synthesis of highly re-dispersible natural polymer capped silver nanoparticles. *Radiation Physics and Chemistry*, *79*, 1240–1246.

Renard, D., Lavenant-Gourgeon, L., Ralet, M. C., & Sanchez, C. (2006). Acacia senegal gum: continuum of molecular species differing by their protein to sugar ratio, molecular weight, and charges. *Biomacromolecules*, *7*, 2637–2649.

Rodd, A. B., Cooper-white, J. J., Dunstan, D. E., & Boger, D. V. (2001a). Gel point studies for chemically modified biopolymer networks using small amplitude oscillatory rheometry. *Polymer*, *42*, 185–198.

Rodd, A. B., Cooper-white, J. J., Dunstan, D. E., & Boger, D. V. (2001b). Polymer concentration dependence of the gel point for chemically modified biopolymer networks using small amplitude oscillatory rheometry. *Polymer*, *42*, 3923–3928.

Sandolo, C., Matricardi, P., Alhaique, F., & Coviello, T. (2009). Effect of temperature and cross-linking density on rheology of chemical crosslinked guar gum at gel point. *Food hydrocolloids*, *23*, 210–220.

Sharma, V. K., Yongard, R. A., & Lin, Y. (2009). Silver nanoparticles: Green synthesis and their antimicrobial activities. *Advances in Colloid and Interface Science*, *145*, 83–96.

Thomas, V., Mohan, Y. M., Sreedhar, B., & Bajpai, S. K. (2009). Fabrication, characterisation of chitosan/nanosilver film and its potential antibacterial application. *Journal of Biomaterial Science Part A: Polymer Edition*, *20*, 2129–2144.

Thomas, V., Namdeo, M., Mohan, Y. M., Bajpai, S. K., & Bajpai, M. (2008). Review on polymer hydrogel and microgel metal nanocomposites: A facile nanotechnological approach. *Journal of Macromolecular Science Part A: Pure Applied Chemistry*, *45*, 107–119.

Varaprasad, K., Mohan, Y. M., Vimala, K., & Raju, K. M. (2011). Synthesis and characterization of hydrogel–silver nanoparticle–curcumin composites for wound dressing and antibacterial application. *Journal of Applied Polymer Science*, *121*, 784–796.

Varshney, L. (2007). Role of natural polysaccharides in radiation formation of PVA–hydrogel wound dressing. *Nuclear Instruments and Methods in Physics Research B*, *255*, 343–349.

Vimala, K., Mohan, Y. M., Varaprasad, K., Reddy, N., Narayana Ravindra, S., Naidu, N. S., et al. (2011). Fabrication of curcumin encapsulated chitosan–PVA silver nanocomposite films for improved antimicrobial activity. *Journal of Biomaterials and Nanobiotechnology*, *2*, 55–64.

Vimala, K., Sivudu, K. S., Mohan, Y. M., Sreedhar, B., & Raju, K. M. (2009). Controlled silver nanoparticle synthesis in semi-hydrogel networks of poly(acrylamide) and carbohydrates: A rational methodology for antibacterial application. *Carbohydrate polymers*, *75*, 463–471.